PONTIFICIA UNIVERSIDAD CATÓLICA DEL ECUADOR

FACULTAD DE CIENCIAS EXACTAS Y NATURALES

ESCUELA DE CIENCIAS BIOLÓGICAS

Description and phylogenetic relationships of a new species of treefrog of the *Osteocephalus buckleyi* species group (Anura: Hylidae)

Disertación previa a la obtención del título de Licenciada en

Ciencias Biológicas

VALERIA DENNISSE CHASILUISA PINCAY

QUITO, 2019

A mi familia

Description and phylogenetic relationships of a new species of treefrog of the *Osteocephalus buckleyi* species group (Anura: Hylidae)

Valeria D. Chasiluisa. Museo de Zoología, Escuela de Biología, Pontificia Universidad Católica del Ecuador, Av. 12 de Octubre y Roca, Aptdo. 17-01-2184. Quito, Ecuador.

Santiago R. Ron. Museo de Zoología, Escuela de Biología, Pontificia Universidad Católica del Ecuador, Av. 12 de Octubre y Roca, Aptdo. 17-01-2184. Quito, Ecuador.

Abstract

The *Osteocephalus buckleyi* species group is widely distributed in primary and secondary forests of South America. Based on integrative analysis, including morphological and genetic data, we estimate the phylogenetic relationships and species boundaries among populations of the *Osteocephalus buckleyi* group from the Ecuadorian Amazon, focusing on the *O. verruciger-O. cannatellai* species complex. Our results uncovered the existence of one confirmed candidate species from Sangay National Park and one unconfirmed candidate species. Here, we describe the new species which is morphologically and ecologically distinct from other *Osteocephalus* species. The new species is unusual because it shows quite distinct morphology, but low genetic distances compared to its closest relatives.

Keywords: *Osteocephalus*, molecular tools, new species, biodiversity, Ecuador.

Introduction

The genus *Osteocephalus* Steindachner 1862 is widely distributed in South America, from Venezuela, Guianas, and the Amazon basin to central Bolivia, and from the eastern Andean slopes of Bolivia to Colombia (Frost, 2018). It's distributed from 0 to 2000 m.a.s.l., in primary and secondary forests (Duellman & Trueb, 1971). *Osteocephalus* comprises a total of 26 recognized species (AmphibiaWeb, 2018) classified into five species groups (Jungfer et al., 2013): *O. alboguttatus, O. buckleyi, O. leprieurii, O. planiceps*, and *O. taurinus* species group.

The *Osteocephalus buckleyi* species group includes 13 species: *O. buckleyi* (Goin, 1961), *O. cabrerai* (Duellman & Mendelson, 1995), *O. camufatus* Jungfer et al., 2016, *O. cannatellai* Ron et al., 2012, *O. carri* (Cochran & Goin, 1970), *O. duellmani* Jungfer 2011,

O. festae (Peracca, 1904), *O. germani* Ron et al., 2012, *O. helenae* (Ruthven, 1919), *O. mimeticus* (Melin, 1941), *O. mutabor* Jungfer and Hödl, 2002, *O. verruciger* (Werner, 1901), and *O. vilmae* Ron et al., 2012. Eight of these species occur in Ecuador (Ron et al., 2018). One putative morphological synapomorphy for the *O. buckleyi* group is its reproduction, which occurs along streams, where eggs are deposited (Jungfer et al., 2013).

The *Osteocephalus buckleyi* species group was the first formally defined within *Osteocephalus*. It was proposed by Cochran and Goin (1970); one year later, Duellman and Trueb (1971) published the first review of the genus. The most recent reviews of the group carried out by Ron et al. (2012) and Jungfer et al. (2013), revealed that it still has unresolved taxonomic issues due, to among others the presence of undescribed species because of similar morphology between species and the presence of cryptic species. In this study, we focus on evaluated the species limits within *O. verruciger* and *O. cannatellai* clades, and describe a new species discovered during an expedition to Sangay National Park, in Amazonian slopes of the Andes of Ecuador. We also present a new phylogeny for *Osteocephalus*, focusing on the *O. buckleyi* species group. The species description is based on an integrative analysis of genetic and morphological data.

Methods

Morphological analyses

We examined alcohol-preserved specimens of the *Osteocephalus buckleyi* group (Appendix 1) deposited at the herpetological collection of the Museo de Zoología at Pontificia Universidad Católica del Ecuador (QCAZ) including the type material of *O. cannatellai* (QCAZ 49572) and one syntype of *Hyla verrucigera* (ZMB 16589) from the National History Museum, Leibniz Institute for Evolutionary and Biodiversity Research in Berlin, Germany.

The format for species diagnosis and description follows Duellman and Trueb (1971). Notation for hand and foot webbing is based on Savage and Heyer (1997). Sex and reproductive status were determined by gonad inspection. Morphometric measurements were taken with a digital caliper (to the nearest 0.01 mm). Adult specimens were measured for the following variables (Duellman, 1970): snout-vent length (SVL); head length (HL); head width (HW); tympanum diameter (TD); femur length (FEL); tibia length (TL); foot length (FL); and eye diameter (ED) (Table 1 and Table 2). Color data in life was based on

digital photos. We analyzed the SVL for adult males and females to determine size differences between species with a Student's *t*-test using the program JMP® 9.01 (SAS institute, 2010).

DNA extraction, amplification, and sequencing

Genomic DNA was extracted from muscle and liver tissue preserved in 95% ethanol using standard phenol-chloroform extraction protocol (Sambrook et al., 1989). Polymerase chain reaction (PCR) was used to amplify partial mitochondrial genes of 12S rRNA, 16S rRNA, NADH dehydrogenase I (ND1), Cytochrome and Oxidase sub-unit I (CO1). PCR amplifications were performed under standard protocols (Appendix 2) and products were purified and sequenced by the Macrogen Sequencing Team (Macrogen Inc., Seoul, Korea).

Phylogenetic analyses

The obtained sequences of five species (*O. cannatellai*, *O. fuscifacies*, *O. mutabor*, *O. verruciger* and *O. vilmae*). were edited, assembled and aligned using the software Geneious 7.1.7. (GeneMatters Corp, Kearse et al., 2012), with default settings for MAFFT multiple Alignment (Katoh & Toh, 2010), for all mitochondrial genes. To determine phylogenetic relationships within the *Osteocephalus buckleyi* species group, we added sequences of five mitochondrial genes 12S, 16S, ND1, CO1 and Cytochrome-b (Cytb) from GenBank (available at: http://www.ncbi.nlm.nih.gov/genbank/) published by Faivovich et al. (2005), Ron et al. (2010), Ron et al. (2012), Jungfer et al. (2013), Moen and Wiens (2009), Moravec et al. (2009), Salducci et al. (2005), and Wiens et al. (2006). As outgroup, we included sequences of *O. yasuni*, *O. leprieurii*, and *O. fuscifacies* based on phylogenies of Jungfer et al. (2013) and Ron et al. (2012). All newly generated sequences and their GenBank accession numbers are listed in table 3. The sequence matrix was imported to Mesquite 3.04 (Maddison & Maddison, 2015) where manual adjustments were made to eliminated gaps and stop codons sequence in different genes.

Because there was a possibility that each of our sampled genes or codon positions in protein-coding genes were shaped by different evolutionary processes, data was partitioned according to gene and codons positions to analyze each partition under separate models of evolution. We used the software PartitionFinder v.2.1.1 (Lanfear et al., 2012) to simultaneously determine the best partition strategy and evolution models for each partition.

Phylogenetic relationships were inferred under maximum likelihood and Bayesian criteria, using GARLI 2.0 (Zwickl, 2006) and MrBayes 3.2.2 (Ronquist et al., 2012), respectively. Maximum likelihood analyses were carried out using default values, except for the control maximum program memory usage (availablememory = 10,000), and the number of generations without topology improvement required for termination (genthreshfortopoterm = 500,000), because of the large dataset. Analyses were terminated at 554,300 generations. We ran a total of 20 independent searches, starting from 10 randomly generated trees (streefname = random) and 10 stepwise addition trees (streefname = stepwise). We evaluated the exhaustiveness of the global search by comparing the final maximum likelihood value among the 10 replicate searches. We considered that the replicate searches were effective in finding the best trees when more than 90% of them had maximum likelihood values within two units of the best global search. Support was evaluated using 100 bootstrap pseudoreplicates under the same configuration parameters used to determine the best tree.

Bayesian inference analyses consisted of four parallel runs using the Monte Carlo Markov Chain (MCMC) algorithm for 6 x 10^6 generations and sampling every 1,000 generations. Each run had four chains (3 hot and one cold), with a temperature of 0.1. Convergence into a stationary distribution and effective sample sizes (ESS) for all parameters were analyzed using Tracer software version 1.6 (Rambaut & Drummond, 2007). We discarded as burn-in 10% of the sampled generations and combined the four runs to summarize the posterior probabilities of nodes in a maximum clade credibility tree. Pairwise genetic uncorrected *p*-distances in the 16S rRNA gene were calculated using MEGA 7 (Kumar et al., 2016) software. This gene has been commonly used to compare divergence between amphibian species (Fouquet et al., 2007; Vieites et al., 2009). We analyzed *p*-distances in the 16S rRNA gene between all species, except for clade G from Colombia (sequences of the 16S gene were not available).

Results

Phylogenetic relationships

The complete DNA sequence matrix contained five mitochondrial genes and up to 4,856 bp for 180 individuals. The software PartitionFinder choose four partitions as the best strategy (best model in parentheses): 12S, 16S, ND1 1st and 3rd position, and CO1 3rd

position (GTR + 1 + G); ND1 2nd position and Cytb 1st position (HKY + I + G); COI 1st position and Cytb 2nd and 3rd position (K80 + I + G); and CO1 2nd position (F81 + I). Topologies of maximum likelihood and Bayesian inference were very similar except for weakly supported nodes (posterior probabilities, pp < 0.96 and bootstrap < 64). Phylogenetic relationships among species of the *Osteocephalus buckleyi* group were consistent with those reported by Ron et al. (2012) and Jungfer et al. (2013).

We found a strongly supported clade for specimens identified as *O. verruciger*, *O. cannatellai*, and the population from Sangay National Park (Fig. 1). These specimens are distributed among seven subclades, all well supported (pp > 0.99; bootstrap > 94) except for clade B (pp = 0.99; bootstrap = 59). Clades A and B form a clade sister to clade C. Clade A includes specimens from Sardinayacu, Sangay National Park, Province of Morona Santiago; its sister clade is composed by *O.* cf. *cannatellai* from southeastern Ecuador (province of Zamora Chinchipe) and northeastern Peru (Cordillera Kampankis); clade C comprises *O. cannatellai* from eastern Ecuador (provinces of Morona Santiago, Napo, Orellana, Pastaza, and Sucumbíos), southeast Colombia (department of Caquetá), and northeastern Peru (department of Loreto) (Fig. 2). The remaining clades (D–G) include individuals traditionally described to *O. verruciger*. Phylogenetic relationships among them are weakly supported (pp < 0.5; bootstrap < 50).

Sequence divergence (uncorrected *p*-distance for gene 16S) within the *O. verruciger-cannatellai* complex (clades A to F) is low and ranges from 0.7 to 1.5% among clades and 0 to 0.1% within clades (Table 4). The genetic distance between the Sangay clade (clade A) and its closest relative (Clade B) is only 0.7%. However, the Sangay population shows a quite distinct morphology compared to clades B and C (*O. cannatellai*; see species diagnosis section). Therefore, we conclude that the Sangay population represents a new species that we describe in the following section. The recognition of the new species renders *O. cannatellai* paraphyletic because some populations of *O. cannatellai* are more closely related to the new species than to other populations of *O. cannatellai* (Fig. 1). We discuss the status of both clades in the taxonomic review section.

We found significant size differences (adult males and females) between most clades (Fig. 3). Males of clade A are smaller than those of clades C– F (all *P* values for *t* tests < 0.001), males of clade B are smaller than those of clade C (t = -6.74, df = 29, P < 0.001); clade C has the largest males. Clade F has smaller males than clade D (t = -4.05, df = 29, P <

0.001) and E (t = -3.97, df = 29, P < 0.001). Females of clade A are smaller than those of clades B–F (all P values for t tests < 0.001), females of the other clades (B–F) are similar in size.

Taxonomic review

We examined the holotype of *O. cannatellai* (QCAZ 49572), one syntype of *O. verruciger* (ZMB 16589) (Fig. 4) and published descriptions of types of five species of *Osteocephalus* (*O. festae*, *O. mimeticus*, and *O. mutabor*) to assign the names to clades A–G. We document those assignments in the following section.

Taxonomic status of *Osteocephalus cannatellai*

Based on morphology and phylogenetic position of the holotype of *O. cannatellai*, we assign clade C as *O. cannatellai sensu stricto*. We suggest that Clade B is considered *O.* cf. *cannatellai* until a thorough review of both clades is carried out. Size differences and life-coloration differences suggest that clade B represent a species distinct from *O. cannatellai*.

Taxonomic status of *Osteocephalus verruciger*

The description of *Hyla verrucigera* is based in two syntypes, (ZMB 16589 and ZMH A00946). One syntype (ZMH A00946), is an adult specimen and is lost (Trueb & Duellman, 1970). The type locality is "Ecuador" and the description by Werner (1901) is short (Appendix 3). It was collected in the years 1899–1900 by Rich Haensch, who traveled through seven provinces in Ecuador (Fig. 2) (Haensch, 1903): Bolívar (Balsapamba), Guayas (Palmar), Napo (Ahuano, Archidona, Baeza, Papallacta, and Pucurcu), Orellana (Coca), Pastaza (Canelos, Sarayacu), Pichincha (Santa Inés) and Tungurahua (Baños de Agua Santa). Photographs of one syntype (ZMB 16589) are provided (Fig. 4). This syntype is a young male with faded coloration, so it can not be unambiguously assigned to a specific clade within *O. verruciger*. However, the itinerary of the collector, indicates that the type material should fall within clades D, E, or F (Fig. 2). Trueb and Duellman (1970) examined syntype ZMB 16589 and considered it "nearly identical" to a juvenile from Cordillera del Dué (Sucumbíos province; KU 123186) which should be part of clade F. The description of the syntype by Trueb and Duellman (1970) suggests that it has lost color since they examined it in the 1960s. We tentatively follow

Trueb and Duellman (1970) in considering clade F as *O. verruciger sensu stricto* but note that it could also belong to clades D or E.

Werner (1901) description of *Hyla verrucigera* (Appendix 3) indicates that the lost syntype is an adult female with heavily tuberculated dorsal areas. This is inconsistent with the morphology of adult females of *O. verruciger* because heavy tuberculation is only present on adult males. It is likely that the sex of the syntype reported by Werner was incorrect. No other hylid from the foothill forests in the Amazon basin of Ecuador fits Werner (1901) description of a heavily tuberculated dorsum. Therefore, we consider highly unlikely that the syntype belongs to a different species of hylid.

Systematic accounts

***Osteocephalus sangay* sp. n.**

Common name. Proposed standard English name: Sangay casqued treefrog. Proposed standard Spanish name: Rana de casco del Sangay.

Holotype. (Fig. 5) QCAZ 58832 (field no. SC-PUCE 48058), adult female from Ecuador, Morona Santiago Province, Sangay National Park, Sardinayacu, Refuge 2 (2.0903°S, 78.1897°W), 1551 m above sea level, collected by Daniel Rivadeneira, Francy Mora, Juan Carlos Sánchez, and Andrea Correa on 18 January 2015.

Paratypes: ECUADOR: MORONA SANTIAGO PROVINCE: Sangay National Park, Sardinayacu: Laguna Chimerella (2.0885°S, 78.2069°W) 1650 m, QCAZ 58829 (subadult female), 58839 (adult female), 58840 (adult male), same date and collectors as the holotype; Refuge 2 (2.0903°S, 78.1897°W), 1551 m, QCAZ 58834 (juvenile male), same date and collectors as the holotype; Refuge 3 (2.0737°S, 78.2184°W), 1795 m, QCAZ 58823–58825 (adult females), collected by J. Pinto, D. Velalcázar, and D. Nuñez on 18 January 2015; Refuge 3, path to Refuge 2 (2.0757°S, 78.2157°W), 1724 m, QCAZ 59124 (adult male), 59125 (adult female), collected by S. Ron, D. Paucar, P. Venegas, P. Baldeón, M. Caminer, and E. Nusirquia on 28 February 2015 (Fig. 5).

Diagnosis: the diagnosis and comparisons are based on six adult females and two adult males. Coloration corresponds to live individuals. *Osteocephalus sangay* sp. n. can be diagnosed by the following characters: (1) mean SVL 40.82 mm in males (range 40.32–41.31; $n = 2$), 49.65 mm in females (range 46.68–52.82; $n = 6$); (2) skin on dorsum bearing

keratinized tubercles in males and scattered tubercles in females; (3) skin on flanks areolate; (4) hand webbing formula varying from I basal II1$^{2}/_{3}$–3^{+}III2$^{2}/_{3}$–2$^{1}/_{3}$IV to I basal II2–3$^{1}/_{3}$III2$^{2}/_{3}$–2$^{1}/_{2}$IV; foot webbing formula varying from I1$^{2}/_{3}$–2^{-}II1^{+}–2III1^{-}–2^{-}IV2^{-}–1^{-}V to I1$^{1}/_{2}$–2+II1+–2$^{1}/_{3}$III1$^{1}/_{3}$–2+IV2-–1-V; (5) dorsum light to medium brown with irregular dark brown marks; (6) venter varying from cream to tan with dark brown dots; (7) cream suborbital mark present; irregular black labial stripe; (8) flanks cream with darker reticulations and brown blotches dorsally; (9) dermal roofing bones of the skull weakly exostosed; (10) bones green in life; (11) iris bronze with irregular black reticulations and olive green ring around the pupil; (12) paired lateral vocal sacs, behind jaw articulation; (13) larvae unknown.

Description of holotype: adult female, 52.39 mm SVL, head length 17.95, head width 15.79, eye diameter 4.35, tympanum diameter 4.15, femur length 25.44, tibia length 27.23, foot length 22.02. Head narrower than body; slightly longer than wide; snout truncate in lateral and dorsal views; distance from nostril to eye longer than diameter of eye; canthus rostralis rounded; loreal region concave; internarial region depressed; nostrils moderately protuberant; interorbital area slightly concave; eye large, protuberant; tympanum rounded, separated from eye by ca. one time its diameter; tympanic membrane evident; supratympanic fold thin, posterior end not reaching arm insertion. Thin arm; axillary membrane present; ulnar tubercles absent; relative length of fingers I < II < IV < III; fingers bearing large, oval discs; subarticular tubercles prominent, round to ovoid; single; supernumerary tubercles present; palmar tubercle small and round; prepollical tubercle large, elliptical; prepollex enlarged; fingers webbing formula I basal II2-–3+III3–2$^{1}/_{2}$IV (Fig. 6). Toes bearing expanded discs, smaller than those of fingers; relative length of toes I < II < V < III < IV; outer metatarsal tubercle present, round; inner metatarsal tubercle present, ovoid, protuberant; supernumerary tubercles present; toes webbing formula I1$^{2}/_{3}$–2$^{1}/_{3}$II1+–2III1+–2-IV2-–-V; skin on dorsum, head and dorsal surfaces of limbs with tubercles; skin on flanks areolate; skin on venter and ventral surfaces of thighs granular, ventral surfaces of shanks smooth. Cloacal opening directed posteriorly at upper level of thighs, round tubercles below vent. Tongue cordiform, widely attached to the mouth floor; dentigerous processes of vomers angular, behind level of ovoid choanae, each bearing 8 and 10 (left/right) vomerine teeth.

Color of holotype in life: Based on digital photographs (Fig. 7). Dorsum light to medium brown with irregular dark brown marks; dorsal surfaces of forearms brown with few dark brown marks; dorsal surfaces of thighs, shanks, and feet light to medium brown with dark brown irregular flecks. Head with one big dark brown irregular blotch; sides of head brown with an oblique cream to tan bar from posteroventral border of orbit to the middle of jaw, below tympanum; tympanum medium brown; flanks cream to tan with dark brown reticulations and irregular dark brown blotches anteriorly; dorsal surfaces of thighs, shanks and forelimbs light to medium brown with dark brown flecks. Venter cream to tan with dark brown dots; olive green ring around the pupil; bronze iris with black reticulations.

Color of holotype in preservative: Dorsum brown with dark brown irregular blotches; a big dark brown blotch in the head between orbits to the flank; dorsal surfaces of forearms and thighs brown with dark brown and light brown flecks; dorsal surfaces of shanks and feet light brown with small brown flecks; flanks light cream with irregular blotches; venter light cream with light brown spots, more abundant in the anterior half of the body; ventral surfaces of hindlimbs and forelimbs light to medium brown; sides of head light brown with a light cream bar from posteroventral border of orbit to middle of jaw, below tympanum; iris gray with black irregular reticulations (Fig. 5).

Variation: In life, based on digital photographs (Fig. 7), adult male (QCAZ 58840) with dorsal olive green coloration and keratinized tubercles, canthal region green with cream subocular mark, tympanum light green; flanks light green to cream with dark brown reticulation; venter cream. In adult females (QCAZ 58825 and 58839) dorsal coloration is the same as in preserved specimens, tympanum light brown, flanks light brown with dark brown reticulation and irregular dark brown blotches posteriorly. Canthal region brown with a cream tan (QCAZ 58839) to light yellow (QCAZ 58825) subocular mark; venter tan with brown reticulation in QCAZ 58839, and cream with a little light brown reticulation in QCAZ 58825.

In preservative (Fig. 5), dorsal background coloration varies from light brown (QCAZ 59125) to dark brown (QCAZ 58825), with irregular dark brown blotches. Young and adult males bear keratinized tubercles (QCAZ 58840 and QCAZ 59124), which are scattered in females (QCAZ 58824). Ventral surfaces of preserved specimens vary from light cream (QCAZ 58825 and QCAZ 59125) to tan with dark brown dots (QCAZ 58839).

Comparisons with other species: *Osteocephalus sangay* is most similar to *O. fuscifacies*. Both species are similar in having brown to dark brown dorsal skin (females of *O. sangay*) and bronze iris with thin black reticulation in life. *Osteocephalus sangay* differs from *O. fuscifacies* in having: (1) dorsum with prominent and abundant tubercles in males, scattered tubercles in females (dorsum smooth in *O. fuscifacies*); (2) dorsal surfaces of limbs with irregular dark brown blotches (dark brown bars with light edges in *O. fuscifacies*); (3) a cream subocular mark (absent in *O. fuscifacies*); and (4) skin on flanks areolate (smooth in *O. fuscifacies*). Mitochondrial DNA sequences show that *O. sangay* and *O. fuscifacies* belong to different species groups.

Osteocephalus sangay is similar to *O. verruciger*, both species share skin tubercles in males and females. *Osteocephalus sangay* differs from *O. verruciger* in having: (1) bronze iris with black reticulations (brown iris without reticulations in *O. verruciger*); (2) irregular blotches in dorsum and dorsal surfaces of forearms and thighs (absent in *O. verruciger*); (3) cream to tan venter with brown reticulation (dark brown mottled venter in *O. verruciger*); and (4) ventral surfaces of forearms and thighs light to brown (reddish brown in *O. verruciger*) (Trueb & Duellman, 1970). *Osteocephalus sangay* is most closely related to *O. cannatellai* from which it differs in having: (1) brown dorsum in females, olive green in males (green dorsum with dark brown blotches in males and females of *O. cannatellai*); (2) dorsal tubercles in males and females (scattered tubercles in males, smooth skin in females in *O. cannatellai*); (3) inconspicuous tubercles in tarsus (prominent tubercles in *O. cannatellai*); (4) iris without a middle band (dark brown band present in *O. cannatellai*); and (5) smaller size in females (SVL in females of *O. sangay* 49.04 mm (range 45.3–52.8; *n* = 7), SVL in *O. cannatellai* 66.5 mm (range 62.6–72.8; *n* = 33) (Ron et al., 2012).

Osteocephalus sangay differs from *O. taurinus* in having a bronze iris with black irregular reticulation (golden iris with thick black lines radiating from the pupil in *O. taurinus*) and smaller body size in males and females (69.4–76.2 mm, n = 4; 64.2–94.1 mm, n = 9 in *O. taurinus*) (Ron 2001–2011). *Osteocephalus festae* can be distinguished from *O. sangay* in having: (1) cream venter with chocolate blotches (venter without blotches in *O. sangay*); (2) cream thin labial stripe (irregular black labial stripe in *O. sangay*) (Ron et al., 2010); and (3) brown iris. *Osteocephalus sangay* differs from *O. mutabor* in having irregular blotches in dorsum and limbs (dark brown transversal bars in dorsum and limbs in *O. mutabor*) and lacks cream lines on heels and vent (present in *O. mutabor)* (Jungfer & Hödl,

2002). *Osteocephalus mimeticus* differs from *O. sangay* in having black iris with some golden blotches and adult males with dorsal yellow brown blotches (lack in adult males of *O. sangay*) (Jungfer, 2010).

Distribution and ecology: *Osteocephalus sangay* is known from eastern Ecuador, Morona Santiago province, Sangay National Park, at four nearby localities (maximum distance between localities: 3.7 km), and elevations between 1551 and 1795 m above sea level. *Osteocephalus sangay* occurs sympatrically with *O. verruciger* at the type locality (Fig. 2). This region corresponds to Eastern Montane Forest (based on Ron et al., 2018 classification). Specimens were found at night in primary *terra firme* forest, perching on vegetation up to 2 m above the ground.

Etymology: The specific epithet *sangay* refers to the area where the species was discovered: Sangay National Park, in Morona Santiago province. The park has more than 3220 lakes and three volcanoes: Sangay, Tungurahua and Altar. The word sangay originates from the native-American Shuar word "Samkay" that means to scare, in reference to violent explosions of this volcano. Sangay National Park is one of the most amphibian species-rich national parks in the world with a total of 100 species (Ron et al. 2019).

Discussion

Our genetic and morphological results document the existence of an undescribed species of *Osteocephalus* from Sangay National Park in Ecuador. The new phylogeny for *Osteocephalus* is consistent with phylogenies published by Ron et al. (2012) and Jungfer et al. (2013). We found strong support for a clade that closely allies *O. verruciger* and *O. cannatellai*. Our results indicate that this clade is a species complex composed of seven clades. We were able to confirm the species status of one of them, *Osteocephalus sangay*. Clade B, sister to the new species, presents a geographic distribution, morphological and molecular differences that suggest it could be an undescribed species masked within "*O. cannatellai*". Nevertheless, more data is needed to better assess variation within *O. cannatellai* and solve the taxonomic status of clade B.

Our study found paraphyly among populations of *O. verruciger* (also reported by Ron et al., 2010 but in contrast with Ron et al., 2012, and Jungfer et al., 2013). Ron et al. (2010) hypothesized that paraphyly could be a result of incomplete lineage sorting, mitochondrial

gene capture or the existence of undescribed species within *O. verruciger*. In our phylogeny, each of the clades of *O. verruciger* is well supported (Fig. 1), and genetic distances between clades vary from 0.7 to 1.1% (uncorrected *p*-distance for 16S), showing differentiation between clades. More morphological and genetic data from a larger number of populations is needed to solve the status of *O. verruciger* and describe putative cryptic species.

Within the *O. verruciger*-*O. cannatellai* complex we found low genetic divergence (less than 1.7% uncorrected *p*-distance for 16S). Previous studies have shown that sister species of hylids are usually separated by higher distances for 16S gene (e.g., Vieites et al., 2009 in *Boophis majori* and *B.* aff. *mayori*, 2.5%; Caminer & Ron, 2014 in *Boana alfaroi* and *B. tetete*, 2.8%; Coloma et al., 2012 in *Hyloscirtus pacha* and *H. criptico*, 3.8%). Our results suggest that species of the *O. verruciger*-*O. cannatellai* complex have unusually low genetic differentiation, a pattern that could arise by recent speciation under divergent selection. However, the fact that *Osteocephalus sangay* occurs in sympatry with *O. verruciger* (clade D), despite being separated by only 1.1% (16S DNA) of genetic distance, indicates that reproductive barriers can evolve even at low levels of genetic differentiation. The existence of reproductive barriers in sympatry is demonstrated by the existence of marked morphological differences *O. sangay* and *O. verruciger* without intermediate morphs.

The elevation range of *O. sangay* (1551–1795 m.a.s.l) overlaps with that of *O. verruciger* (1400–2000 m.a.s.l) and differs from the elevation range of *O. cannatellai* (200–910 m.a.s.l.) and *O.* cf. *cannatellai* (310–1240 m.a.s.l). Non-overlapping altitudinal ranges suggest that divergent selection along the altitudinal gradient played an important role in speciation of these frogs, as previously hypothesized for Andean amphibians by Graham et al. (2004), Salerno et al. (2012) and Ron et al. (2012).

Acknowledgments

This research was funded by the Secretaría de Educación Superior, Ciencia, Tecnología e Innovación del Ecuador SENESCYT (Arca de Noé Initiative; Omar Torres and Santiago R. Ron principal investigators) and Pontificia Universidad Católica del Ecuador. We thank Ana Belén Carrillo and Claudia Terán to carried out laboratory work. Frank Tillack

provided photographs of the syntype of *H. verrucigera*. For field assistance we thank Daniel Rivadeneira, Francy Mora, Juan Carlos Sánchez, Javier Pinto, David Velalcázar, Andrea Correa, Darwin Nuñez, Santiago Ron, Diego Paucar, Pablo Venegas, Pamela Baldeón, Marcel Caminer, and Eloy Nusirquia. We specially thank Marcel Caminer, Diego Ortiz and Andrea Varela for comments on the manuscript and to the personal of Museo de Zoología QCAZ.

References

AmphibiaWeb. (2018). AmphibiaWeb: information on amphibian biology and conservation. https://amphibiaweb.org. University of California, Berkeley, CA, USA. Accessed 15 Dic 2018.

Caminer, M. A., & Ron, S. R. (2014). Systematics of treefrogs of *the Hypsiboas calcaratus* and *Hypsiboas fasciatus* species complex (Anura, Hylidae) with the description of four new species. *Zookeys*, *370*, 1–68. doi: 10.3897/zookeys.370.6291

Cochran, D. M., & Goin, C. J. (1970). Frogs of Colombia. *Bulletin of the United States National Museum, 288*, 1–655.

Duellman, W. E. (1970). Hylid frogs of Middle America. *Monograph of the Museum of Natural History, the University of Kansas*, *1*, 1–753.

Duellman, W. E., & Trueb, L. (1971). Synopsis of Neotropical Hylid Frogs, Genus *Osteocephalus*. *Occasional papers of the Museum of Natural History, the University of Kansas*,*1*, 1–47.

Duellman, W. E., & Mendelson, J. R. (1995). Amphibians and reptiles from northern Departamento Loreto, Peru: taxonomy and biogeography. *University of Kansas. Science Bulletin, 55*, 329–376.

Faivovich, J., Haddad, C. F., Garcia, P. C., Frost, D. R., Campbell, J. A., & Wheeler, W. C. (2005). Systematic review of the frog family Hylidae, with special reference to Hylinae: phylogenetic analysis and taxonomic revision. *Bulletin of the American Museum of natural History*, 1–240.

Folmer, O., Black, M., Hoeh, W., Lutz, R., & Vrijenhoek, R. (1994). DNA primers for amplification of mitochondrial cytochrome c oxidase subunit I from diverse metazoan invertebrates. *Molecular Marine Biology and Biotechnology, 3*(5), 294–299.

Fouquet, A., Gilles, A., Vences, M., Marty, C., Blanc, M., & Gemmell, N. J. (2007). Underestimation of species richness in Neotropical frogs revealed by mtDNA analyses. *PLoS one*, *2*(10), e1109. doi: doi.org/10.1371/journal.pone.0001109

Frost, D. R. (2018). Amphibian Species of the World: an Online Reference. Version 6.0 (15/12/2018). http://research.amnh.org/herpetology/amphibia/index.html. American Museum of Natural History, New York, USA. Accessed 15 Dic 2018.

Goebel, A. M., Donnelly, J. M., & Atz, M. E. (1999). PCR primers and amplification methods for 12S ribosomal DNA, the control region, cytochrome oxidase I, and cytochromebin bufonids and other frogs, and an overview of PCR primers which have amplified DNA in amphibians successfully. *Molecular Phylogenetics and Evolution*, *11*(1), 163–199.

Goin, C. J. (1961). Synopsis of the genera of hylid frogs. *Annals of the Carnegie Museum*, *36*, 5–18.

Graham, C. H., Ron, S. R., Santos, J. C., Schneider, C. J., & Moritz, C. (2004). Integrating phylogenetics and environmental niche models to explore speciation mechanisms in dendrobatid frogs. *Evolution*, *58*(8), 1781–1793.

Haensch, R. (1903). Kurzer Bericht über die entomolog. Ergebnisse meiner Ecuador-Reise. *Berliner Entomologische Zeitschrift*, *48*(3), 149–156. doi:10.1002/mmnd.19030480304

Hedges, S. B., Duellman, W. E., & Heinicke, M. P. (2008). New World direct-developing frogs (Anura: Terrarana): molecular phylogeny, classification, biogeography, and conservation. *Zootaxa*, *1737*(1), 1–182.

Jungfer, K. H. & Hödl, W. (2002). A new species of *Osteocephalus* from Ecuador and a redescription of *O. leprieurii* (Duméril & Bibron, 1841) (Anura: Hylidae). *Amphibia-Reptilia*, *23*(1), 21–46.

Jungfer, K. H. (2010). The taxonomic status of some spiny-backed treefrogs, genus *Osteocephalus* (Amphibia: Anura: Hylidae). *Zootaxa*, *2407*, 28–50.

Jungfer, K. H. (2011). A new tree frog of the genus *Osteocephalus* from high altitudes in the Cordillera del Cóndor, Ecuador (Amphibia: Anura: Hylidae). *The Herpetological Journal*, *21*(4), 247–253.

Jungfer, K. H., Faivovich, J., Padial, J. M., Castroviejo-Fisher, S., Lyra, M. L., Berneck, B. V. M., Iglesias, P. P., Kok, P. J. R., MacCulloch, R. D., Rodrigues, M. T., Verdade, V. K., Torres Gastello, C. P., Chaparro, J. C., Valdujo, P. H., Reichle, S., Moravec, J., Gvoždík, V., Gagliardi-Urrutia, G., Ernst, R., De la Riva, I., Means, D. B., Lima, A. P., Señaris, J. C., Wheeler, W. C., & Haddad, C. F. B. (2013). Systematics of spiny-backed treefrogs (Hylidae: *Osteocephalus*): an Amazonian puzzle. *Zoologica Scripta*, *42*(4), 351–380.

Jungfer, K. H., Verdade, V. K., Faivovich, J., & Rodrigues, M. T. (2016). A new species of spiny-backed treefrog (*Osteocephalus*) from Central Amazonian Brazil (Amphibia: Anura: Hylidae). *Zootaxa*, *4114*(2), 171–181.

Katoh, K., & Toh, H. (2010). Parallelization of the MAFFT multiple sequence alignment program. *Bioinformatics*, *26*(15), 1899–1900.

Kearse, M., Moir, R., Wilson, A., Stones-Havas, S., Cheung, M., Sturrock, S., & Thierer, T. (2012). Geneious Basic: an integrated and extendable desktop software platform for the organization and analysis of sequence data. *Bioinformatics*, *28*(12), 1647–1649.

Kok, P. J., MacCulloch, R. D., Means, D. B., Roelants, K., Van Bocxlaer, I., & Bossuyt, F. (2012). Low genetic diversity in tepui summit vertebrates. *Current biology*, *22*(15), R589–R590.

Kumar, S., Stecher, G., & Tamura, K. (2016). MEGA7: molecular evolutionary genetics analysis version 7.0 for bigger datasets. *Molecular biology and evolution*, *33*(7),1870–1874.

Maddison, W. P., & Maddison, D. R. (2015). Mesquite: a modular system for evolutionary analysis. Version 3.04. http://mesquiteproject.org

Melin, D. (1941). Contribution to the knowledge of the Amphibia of South America. Göteborgs Kungl. Vetenskaps-och Vitterhets-samhälles. Handlingar. Serien B, *Matematiska och Naturvetenskapliga Skrifter*, *1*, 1–71.

Moen, D. S., & Wiens, J. J. (2009). Phylogenetic evidence for competitively driven divergence: body-size evolution in Caribbean treefrogs (Hylidae: *Osteopilus*). *Evolution: International Journal of Organic Evolution*, *63*(1), 195–214.

Moravec, J., Aparicio, J., Guerrero-Reinhard, M., Calderón, G., Jungfer, K. H., & Gvoždík, V. (2009). A new species of *Osteocephalus* (Anura: Hylidae) from Amazonian Bolivia: first evidence of tree frog breeding in fruit capsules of the Brazil nut tree. *Zootaxa, 2215*(1), 37–54.

Palumbi, S. R., Martin, A., Romano, S., McMillan, W. O., Stice, L., & Grabowski, G. (1991). The simple fool's guide to PCR, version 2.0. *University of Hawaii, Honolulu*, *45*, 1–24.

Peracca, M. G. (1904). Viaggio del Dr. Enrico Festa nell' Ecuador e regioni vicine. *Bollettino dei Musei di Zoologia ed Anatomia comparata, Università di Torino*, *465*, 1–41.

Rambaut, A., & Drummond, A. J. (2007). Tracer: MCMC trace analysis tool v 1.4. University of Oxford.

Ron, S. R. (2001–2011). Anfibios de Parque Nacional Yasuní, Amazonía ecuatoriana. [en línea]. ver. 1.7 (2011). Museo de Zoología, Pontificia Universidad Católica del Ecuador. Quito, Ecuador.

Ron, S. R., Toral, E., Venegas, P. J., & Barnes, C. W. (2010). Taxonomic revision and phylogenetic position of *Osteocephalus festae* (Anura, Hylidae) with description of its larva. *ZooKeys*, *70*, 67–92. doi: 10.3897/zookeys.70.765

Ron, S. R., Venegas, P. J., Toral, E., Read, M., Ortiz, D. A., & Manzano, A. L. (2012). Systematics of the *Osteocephalus buckleyi* species complex (Anura, Hylidae) from Ecuador and Peru. *ZooKeys, 229*, 1–52. doi: 10.3897/zookeys.229.3580

Ron, S. R., Merino-Viteri, A., & Ortiz, D. A. (2018). Anfibios del Ecuador. Version 2019.0. Museo de Zoología, Pontificia Universidad Católica del Ecuador. < https://bioweb.bio/faunaweb/amphibiaweb>, Accessed 15 Dic 2018

Ronquist, F., Teslenko, M., Van Der Mark, P., Ayres, D. L., Darling, A., Höhna, S., Larget, B., Liu, L., Suchard, M. A., & Huelsenbeck, J. P. (2012). MrBayes 3.2: efficient Bayesian phylogenetic inference and model choice across a large model space. *Systematic biology*, *61*(3), 539–542.

Ruthven, A. G. (1919). The amphibians of the University of Michigan-Walker expedition to British Guiana. *Occasional Papers of the Museum of Zoology, University of Michigan, 69*, 1–14.

Salducci, M. D., Marty, C., Fouquet, A., & Gilles, A. (2005). Phylogenetic relationships and biodiversity in hylids (Anura: Hylidae) from French Guiana. *Comptes Rendus Biologies*, *328*(10–11), 1009–1024.

Salerno, P. E., Ron, S. R., Señaris, J. C., Rojas-Runjaic, F. J., Noonan, B. P., & Cannatella, D. C. (2012). Ancient tepui summits harbor young rather than old lineages of endemic frogs. *Evolution: International Journal of Organic Evolution*, *66*(10), 3000–3013.

SAS Institute (2010). User guide. SAS Institute. Cary. Version 9.01. http://www.jmp.com/.

Savage, J. M., & Heyer, W. R. (1997). Digital webbing formulae for anurans: a refinement. *Herpetological Review, 28*(3), 131.

Steindachner, F. (1862). Über zwei noch unbeschriebene Batrachier aus des Sammlung des KK zoologischn Museum zu Wien. *Archivio per La Zoologia L'Anatomia E La Fisiologia*, *1*, 77–82.

Trueb, L., & Duellman, W. E. (1970). The systematic status and life history of *Hyla verrucigera* Werner. *Copeia*, 601–610.

Vieites, D. R., Wollenberg, K. C., Andreone, F., Köhler, J., Glaw, F., & Vences, M. (2009). Vast underestimation of Madagascar's biodiversity evidenced by an integrative amphibian inventory. *Proceedings of the National Academy of Sciences*, *106*(20), 8267–8272.

Werner, F. (1901). Ueber reptilien und batrachier aus Ecuador und Neu-Guinea. *Verhandlungen des Zoologisch-Botanischen Vereins in Wien, 50*, 593–614.

Wiens, J.J., Fetzner J.W., Parkinson, C.L., & Reeder, T. W. (2005) Hylid frog phylogeny and sampling strategies for speciose clades. *Systematic Biology, 54*, 719–748.

Zwickl, D. J. (2006). *GARLI.* Genetic algorithm approaches for the phylogenetic analysis of large biological sequence datasets under the maximum likelihood criterion (*Doctoral dissertation, Ph. D. dissertation, University of Texas, Austin, Texas, USA*).

Figure legends

Figure 1. Maximum likelihood phylogram depicting relationships within the *Osteocephalus buckleyi* species group. Phylogram derived from analysis of 4,856 bp of mitochondrial DNA (gene fragments 12S, 16S, ND1, CO1 and Cytb). Museum catalog numbers and localities are shown for each sample. Bootstrap values and Bayesian posterior probabilities are shown above and below the branches respectively; missing values indicate values below 50 (bootstrap) or 0.5 (posterior probability). Outgroup species (*O. fuscifacies, O. leprieurii* and *O. yasuni*) are not included. Abbreviations are: **BR** Brazil, **CO** Colombia, **EC** Ecuador, **GU** Guyana, **PE** Peru, **VE** Venezuela.

Figure 2. Distribution of the *Osteocephalus verruciger-O. cannatellai* complex (clades A–G). Localities are based on sequenced specimens from Ecuador, Peru and Colombia deposited at Museo de Zoología of Pontificia Universidad Católica, Centro de Ornitología y Biodiversidad CORBIDI, and Natural History Museum University of Kansas. Black points refers to specific locations visited by Rich Haensch (1903), collector of *O. verruciger* syntypes.

Figure 3. Boxplots for snout-vent length (SVL) from females and males of the *Osteocephalus verruciger-cannatellai* complex. The line in the middle of the box represents the median, and the lower and upper ends of the box are the 25% and 75% quartiles respectively. Letters correspond to those of clades on Figure 1.

Figure 4. Dorsal, lateral and ventral views of the syntype of *Hyla verrucigera (*ZMB 16589). Photographs by Frank Tillack.

Figure 5. Adult preserved specimens of *Osteocephalus sangay* showing variation in dorsal and ventral coloration. From left to right, first and second rows: QCAZ 58832 (holotype), QCAZ 58824, 58839 (females); third and fourth rows: QCAZ 58825, QCAZ 59125 (females), QCAZ 58840, 59124 (males). All specimens are shown at the same scale. Photographs by Valeria Chasiluisa.

Figure 6. Ventral views of the left hand and foot of the holotype of *O. sangay* sp. n. Hand and foot are shown at the same scale. Photographs by Valeria Chasiluisa.

Figure 7. Color variation in life of adult specimens of *Osteocephalus sangay* sp. n. **A–B** QCAZ 58832 (holotype), (SVL = 52.39 mm), adult female; **C–D** QCAZ 58839, (SVL =

52.82 mm), adult female; **E–F** QCAZ 58825, (SVL = 48.40 mm), adult female; **G–H** QCAZ 58840, (SVL = 41.31 mm), adult male.

Figure 8. Dorsal and ventral view of species within the *Osteocephalus verruciger*-*O. cannatellai* complex. **A–B** *Osteocephalus sangay* sp. n., QCAZ 58825, (SVL = 48.40 mm), adult female; **C–D** *O. cannatellai*, QCAZ 67133, (SVL = 62.24 mm), adult female; **E–F** *O.* cf. *cannatellai*, CORDIBI 10534, adult male; **G–H** *O.* cf. *verruciger* (clade D), QCAZ 58827, (SVL = 62.61 mm), adult female; **I–J** *O.* cf. *verruciger* (clade D), QCAZ 58833, (SVL = 47.50 mm), adult male. Photographs by G. Pazmiño, J. C. Sanchez and A. Catenazzi.

Figure 1.

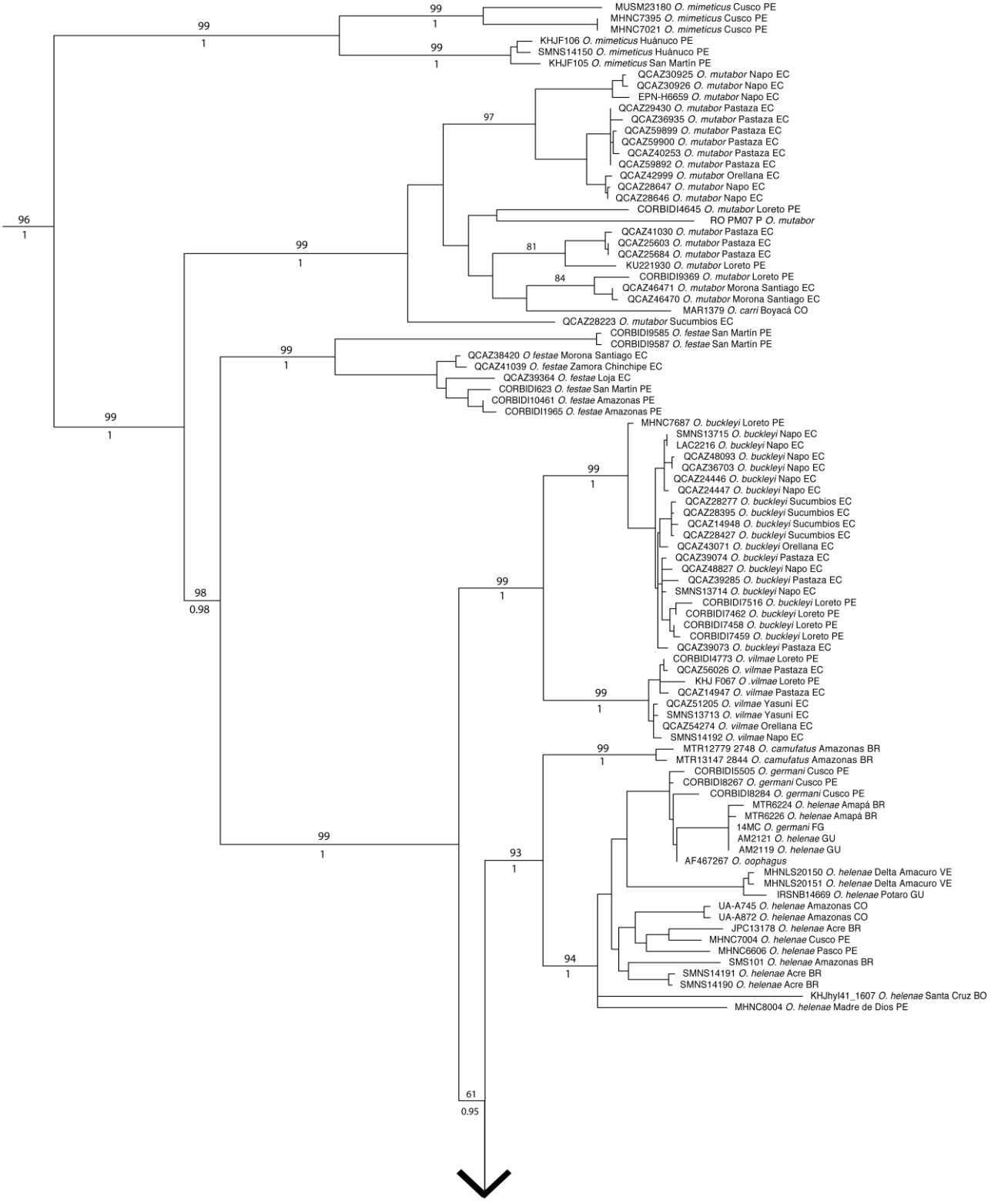
MUSM23180 O. mimeticus Cusco PE
MHNC7395 O. mimeticus Cusco PE
MHNC7021 O. mimeticus Cusco PE
KHJF106 O. mimeticus Huánuco PE
SMNS14150 O. mimeticus Huánuco PE
KHJF105 O. mimeticus San Martín PE
QCAZ30925 O. mutabor Napo EC
QCAZ30926 O. mutabor Napo EC
EPN-H6659 O. mutabor Napo EC
QCAZ29430 O. mutabor Pastaza EC
QCAZ36935 O. mutabor Pastaza EC
QCAZ59899 O. mutabor Pastaza EC
QCAZ59900 O. mutabor Pastaza EC
QCAZ40253 O. mutabor Pastaza EC
QCAZ59892 O. mutabor Pastaza EC
QCAZ42999 O. mutabor Orellana EC
QCAZ28647 O. mutabor Napo EC
QCAZ28646 O. mutabor Napo EC
CORBIDI4645 O. mutabor Loreto PE
RO PM07 P O. mutabor
QCAZ41030 O. mutabor Pastaza EC
QCAZ25603 O. mutabor Pastaza EC
QCAZ25684 O. mutabor Pastaza EC
KU221930 O. mutabor Loreto PE
CORBIDI9369 O. mutabor Loreto PE
QCAZ46471 O. mutabor Morona Santiago EC
QCAZ46470 O. mutabor Morona Santiago EC
MAR1379 O. carri Boyacá CO
QCAZ28223 O. mutabor Sucumbios EC
CORBIDI9585 O. festae San Martín PE
CORBIDI9587 O. festae San Martín PE
QCAZ38420 O festae Morona Santiago EC
QCAZ41039 O. festae Zamora Chinchipe EC
QCAZ39364 O. festae Loja EC
CORBIDI623 O. festae San Martín PE
CORBIDI10461 O. festae Amazonas PE
CORBIDI1965 O. festae Amazonas PE
MHNC7687 O. buckleyi Loreto PE
SMNS13715 O. buckleyi Napo EC
LAC2216 O. buckleyi Napo EC
QCAZ48093 O. buckleyi Napo EC
QCAZ36703 O. buckleyi Napo EC
QCAZ24446 O. buckleyi Napo EC
QCAZ24447 O. buckleyi Napo EC
QCAZ28277 O. buckleyi Sucumbios EC
QCAZ28395 O. buckleyi Sucumbios EC
QCAZ14948 O. buckleyi Sucumbios EC
QCAZ28427 O. buckleyi Sucumbios EC
QCAZ43071 O. buckleyi Orellana EC
QCAZ39074 O. buckleyi Pastaza EC
QCAZ48827 O. buckleyi Napo EC
QCAZ39285 O. buckleyi Pastaza EC
SMNS13714 O. buckleyi Napo EC
CORBIDI7516 O. buckleyi Loreto PE
CORBIDI7462 O. buckleyi Loreto PE
CORBIDI7458 O. buckleyi Loreto PE
CORBIDI7459 O. buckleyi Loreto PE
QCAZ39073 O. buckleyi Pastaza EC
CORBIDI4773 O. vilmae Loreto PE
QCAZ56026 O. vilmae Pastaza EC
KHJ F067 O .vilmae Loreto PE
QCAZ14947 O. vilmae Pastaza EC
QCAZ51205 O. vilmae Yasuní EC
SMNS13713 O. vilmae Yasuní EC
QCAZ54274 O. vilmae Orellana EC
SMNS14192 O. vilmae Napo EC
MTR12779 2748 O. camufatus Amazonas BR
MTR13147 2844 O. camufatus Amazonas BR
CORBIDI5505 O. germani Cusco PE
CORBIDI8267 O. germani Cusco PE
CORBIDI8284 O. germani Cusco PE
MTR6224 O. helenae Amapá BR
MTR6226 O. helenae Amapá BR
14MC O. germani FG
AM2121 O. helenae GU
AM2119 O. helenae GU
AF467267 O. oophagus
MHNLS20150 O. helenae Delta Amacuro VE
MHNLS20151 O. helenae Delta Amacuro VE
IRSNB14669 O. helenae Potaro GU
UA-A745 O. helenae Amazonas CO
UA-A872 O. helenae Amazonas CO
JPC13178 O. helenae Acre BR
MHNC7004 O. helenae Cusco PE
MHNC6606 O. helenae Pasco PE
SMS101 O. helenae Amazonas BR
SMNS14191 O. helenae Acre BR
SMNS14190 O. helenae Acre BR
KHJhyl41_1607 O. helenae Santa Cruz BO
MHNC8004 O. helenae Madre de Dios PE
99
1
99
1
99
1
97
96
1
99
1
81
84
99
1
98
0.98
99
1
99
1
99
1
99
1
99
1
93
1
94
1
61
0.95

Figure 1. Continued.

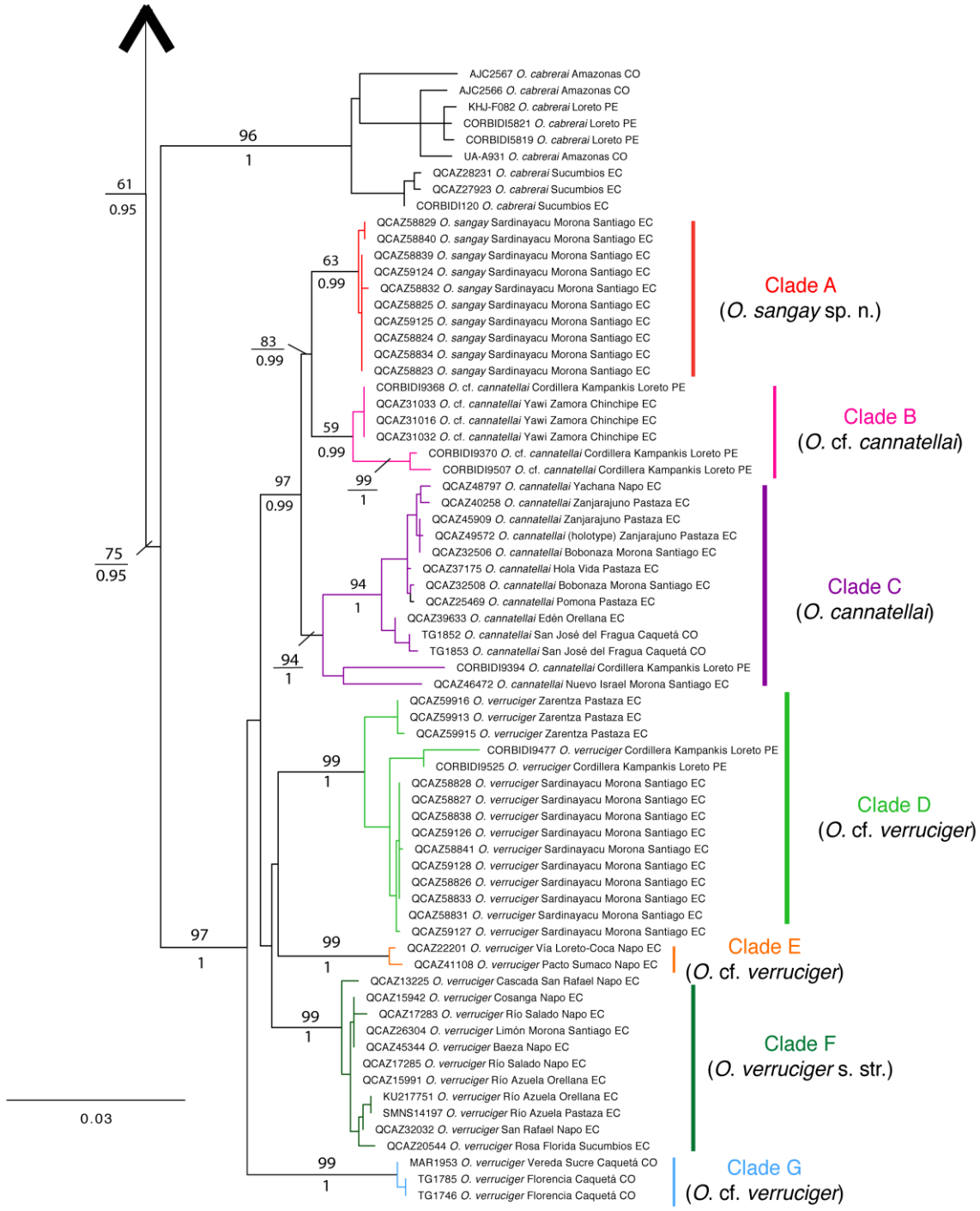

Figure 2.

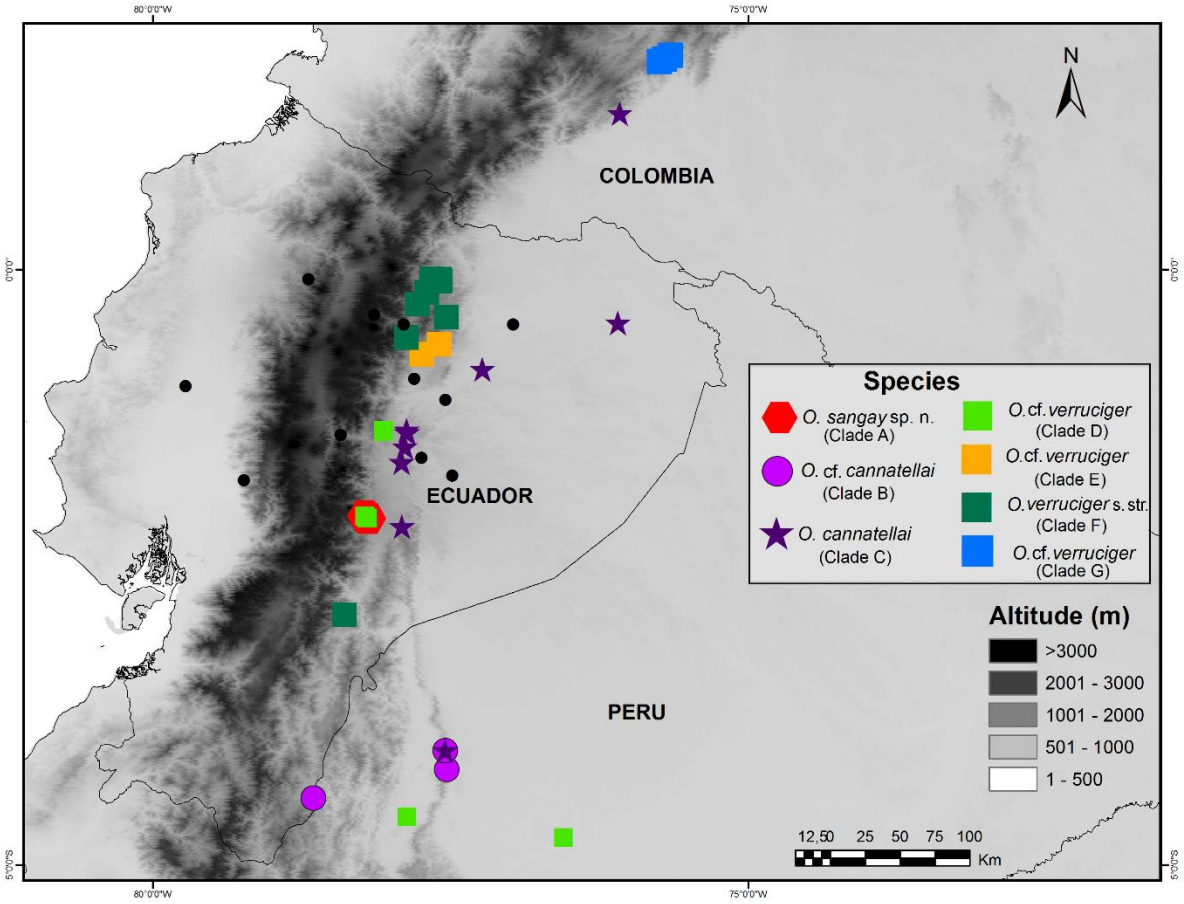
80°0'0"W
75°0'0"W
0°0'0"
5°0'0"S
N
COLOMBIA
ECUADOR
PERU
Species
O. sangay sp. n. (Clade A)
O. cf. cannatellai (Clade B)
O. cannatellai (Clade C)
O. cf. verruciger (Clade D)
O. cf. verruciger (Clade E)
O. verruciger s. str. (Clade F)
O. cf. verruciger (Clade G)
Altitude (m)
>3000
2001 - 3000
1001 - 2000
501 - 1000
1 - 500
12,50 25 50 75 100
Km

Figure 3.

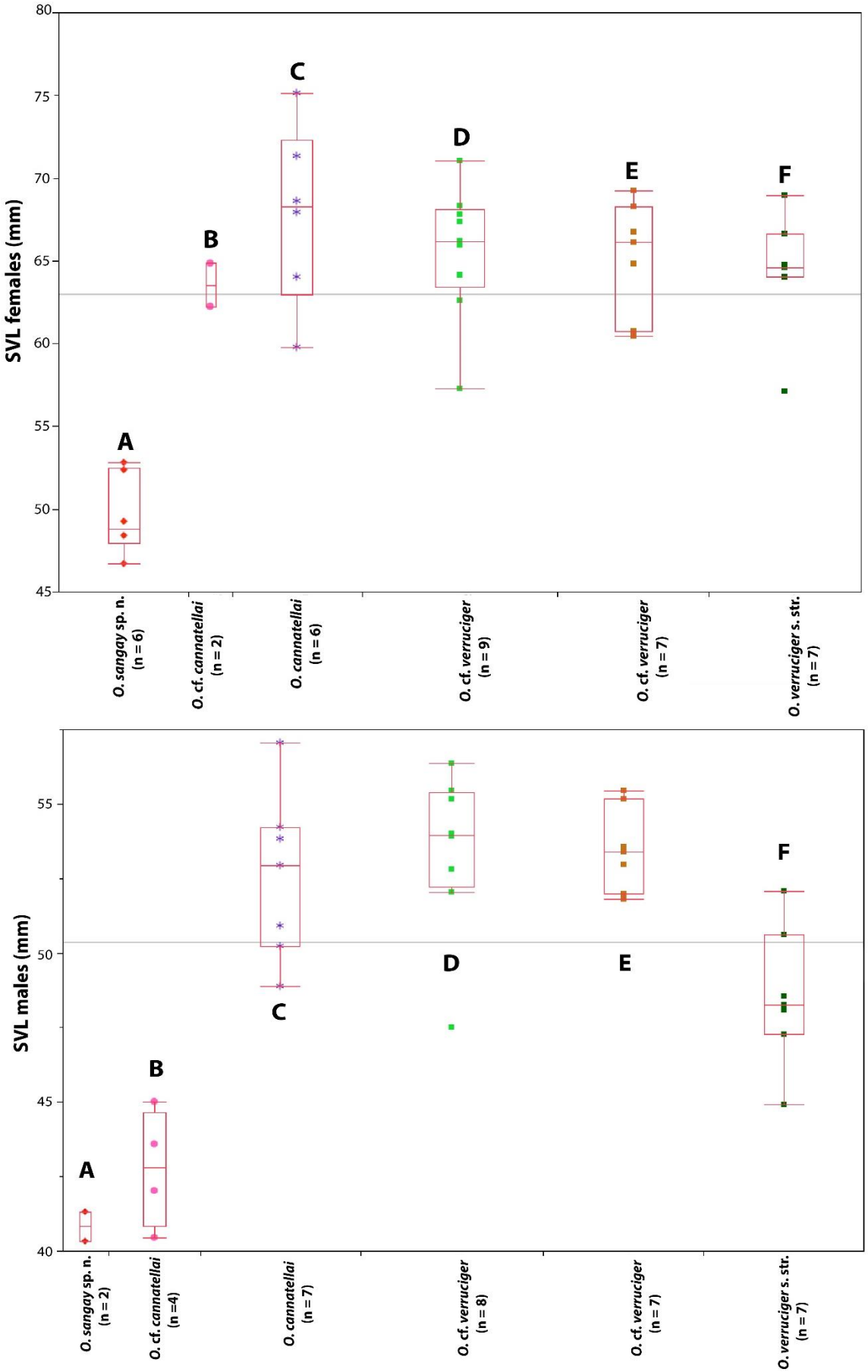
SVL females (mm)
80
75
70
65
60
55
50
45
A
B
C
D
E
F
O. sangay sp. n. (n = 6)
O. cf. cannatellai (n = 2)
O. cannatellai (n = 6)
O. cf. verruciger (n = 9)
O. cf. verruciger (n = 7)
O. verruciger s. str. (n = 7)
SVL males (mm)
55
50
45
40
A
B
C
D
E
F
O. sangay sp. n. (n = 2)
O. cf. cannatellai (n =4)
O. cannatellai (n = 7)
O. cf. verruciger (n = 8)
O. cf. verruciger (n = 7)
O. verruciger s. str. (n = 7)

Figure 4.

Figure 5.

Figure 6.

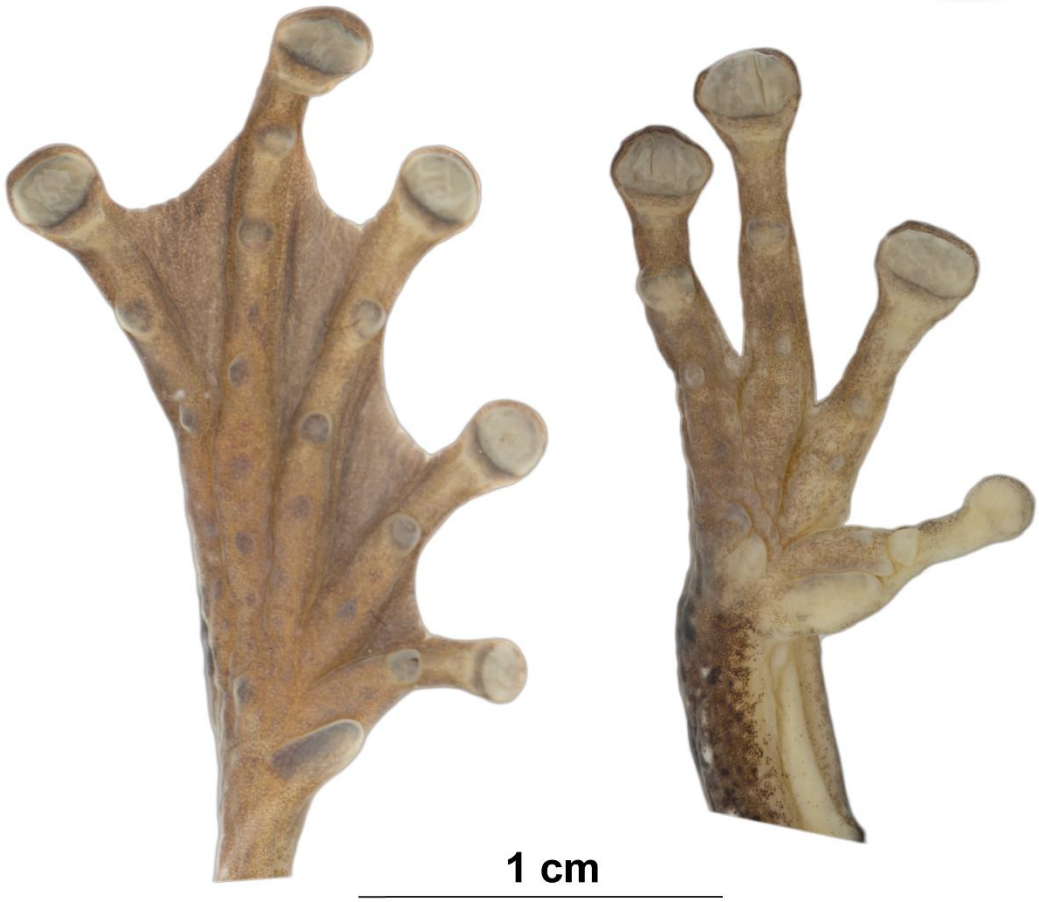

Figure 7.

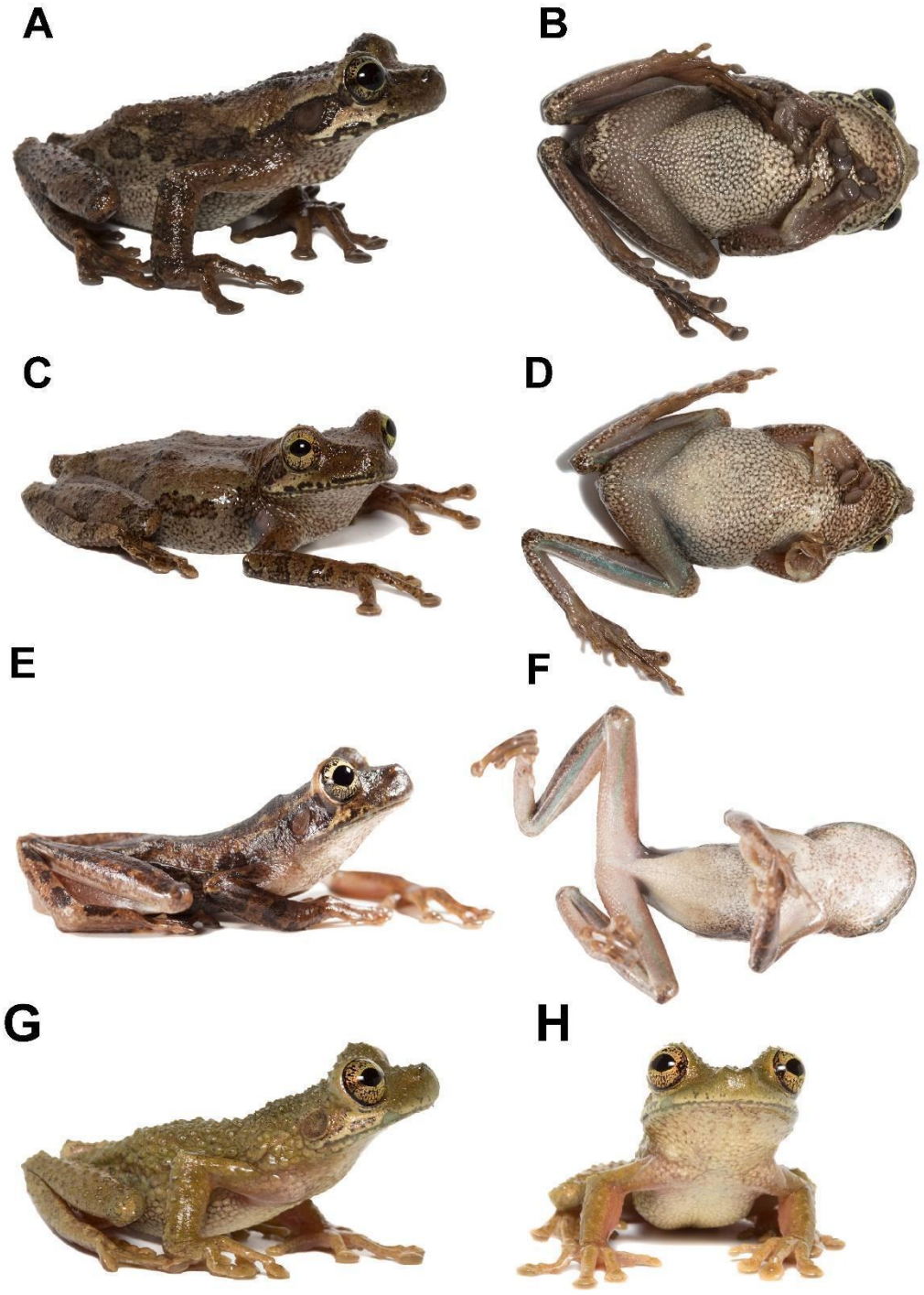

Figure 8.

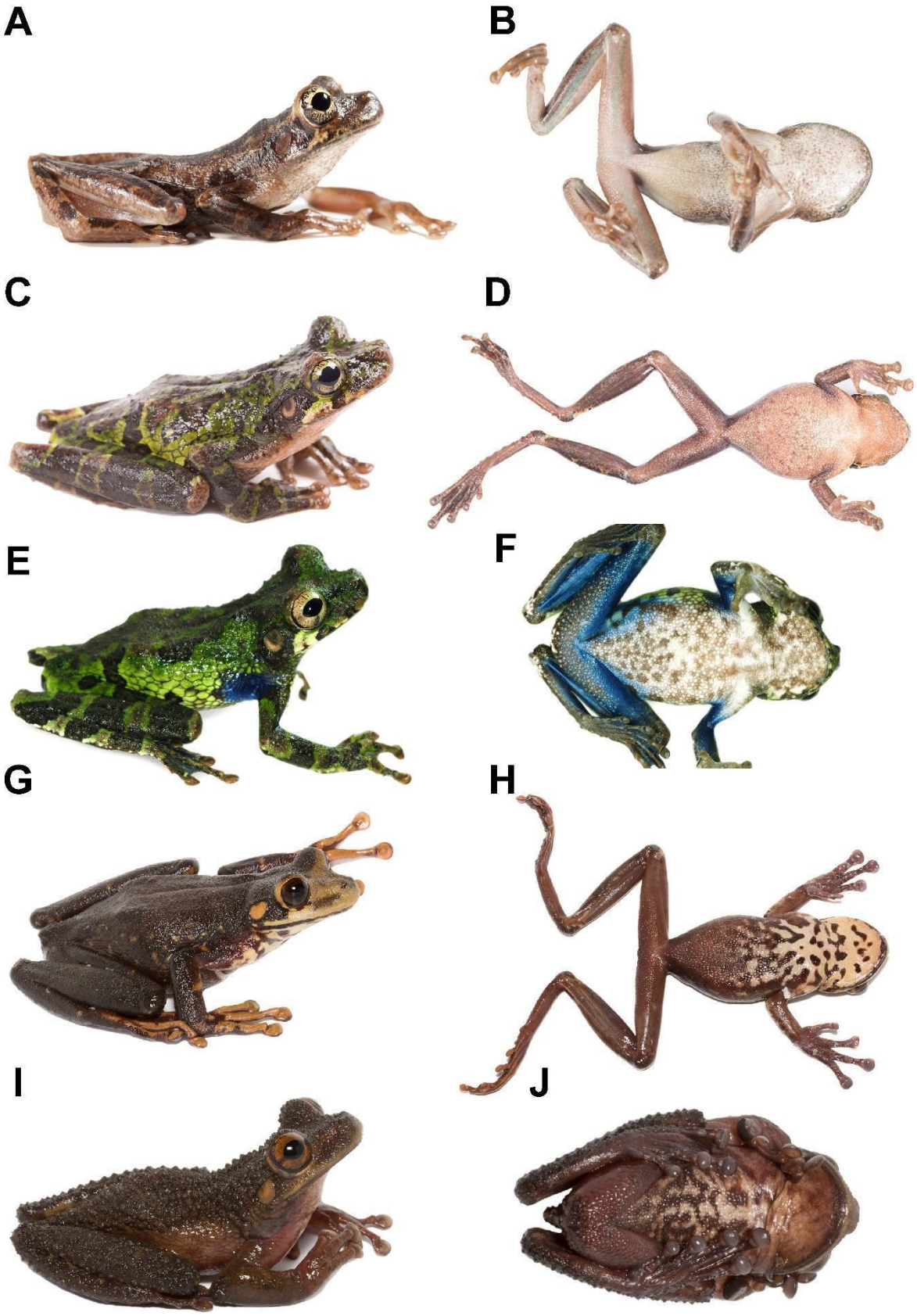

Table 1. Morphological measurements of *Osteocephalus sangay* sp. n. Abbreviations: SVL = snout-vent length; FL = foot length; HL = head length; HW = head width; ED = eye diameter; TD = tympanum diameter; TL = tibia length; FEL = femur length. All measurements in mm.

	Adult female (holotype)	**Adult males (*n* = 2)**	**Adult females (*n* = 5)**	**Subadult female (*n* = 1)**	**Juvenile male (*n* = 1)**
SVL	52.3	40.3–41.3	49.1 ± 2.2 (46.6–52.8)	45.3	36.6
FL	22.0	16.5–16.6	21.0 ± 1.1 (19.4–22.1)	20.3	15.1
HL	17.9	15.2–15.4	17.5 ± 0.6 (16.8–18.4)	16.6	12.7
HW	15.7	13.3–13.4	15.0 ± 0.9 (13.7–16.0)	13.6	11.2
ED	4.3	4.0–4.2	4.0 ± 0.6 (2.9–4.6)	4.3	3.6
TD	4.1	3.0–3.4	3.6 ± 0.3 (3.3–4.2)	3.4	2.7
TL	27.2	20.7–20.8	25.7 ± 1.4 (23.6–27.2)	24.2	19.1
FEL	25.4	19.5–19.6	24.6 ± 1.2 (22.4–25.7)	22.5	17.6

Table 2. Snout-vent length (SVL) measurements of clades A–F. All measurements in mm.

Species	Sex	SVL
O. sangay. sp. n. (Clade A)	Male (*n* = 2)	40.8 ± 0.6 (40.3–41.3)
	Female (*n* = 6)	49.6 ± 2.4 (46.6–52.8)
O. cf. *cannatellai* (Clade B)	Male (*n* = 4)	42.7 ± 1.9 (40.4–45.0)
	Female (*n* = 2)	63.5 ± 1.8 (62.4–64.8)
O. cannatellai (Clade C)	Male (*n* = 7)	52.5 ± 2.7 (48.8–57.0)
	Female (*n* = 6)	67.8 ± 5.3 (59.7–75.1)
O. cf. *verruciger* (Clade D)	Male (*n* = 8)	53.4 ± 2.6 (47.5–56.3)
	Female (*n* = 9)	65.6 ± 3.9 (57.2–71.0)
O. cf. *verruciger* (Clade E)	Male (*n* = 7)	53.4 ± 1.4 (51.7–55.4)
	Female (*n* = 7)	65.1 ± 3.4 (60.4–69.2)
O. verruciger s. str. (Clade F)	Male (*n* = 7)	48.5 ± 2.3 (44.9–52.0)
	Female (*n* = 7)	64.3 ± 3.6 (57.1–68.9)

Table 3. New DNA sequences used in the phylogenetic analysis.

Museum No.	**Species**	**Genbank Accession No.**			
		12S	**16S**	**ND1**	**COI**
QCAZ58832	*Osteocephalus sangay*	To be added	To be added	To be added	To be added
QCAZ58829	*O. sangay*	To be added	To be added	To be added	To be added
QCAZ58840	*O. sangay*	To be added	To be added	To be added	To be added
QCAZ58839	*O. sangay*	To be added	To be added	To be added	To be added
QCAZ59124	*O. sangay*	To be added	To be added	To be added	To be added
QCAZ58825	*O. sangay*	To be added	To be added	To be added	To be added
QCAZ59125	*O. sangay*	To be added	To be added	To be added	To be added
QCAZ58824	*O. sangay*	To be added	To be added	To be added	To be added
QCAZ58834	*O. sangay*	To be added	To be added	To be added	To be added
QCAZ58823	*O. sangay*	To be added	To be added	To be added	To be added
QCAZ48797	*O. cannatellai*	To be added	To be added	To be added	To be added
QCAZ36935	*O. mutabor*	To be added	To be added	To be added	To be added
QCAZ59899	*O. mutabor*	To be added	To be added	To be added	To be added
QCAZ59900	*O. mutabor*	To be added	To be added	To be added	To be added
QCAZ59892	*O. mutabor*	To be added	To be added	To be added	To be added
RO PM07 P	*O. mutabor*	To be added	To be added	To be added	To be added
QCAZ59916	*O. verruciger*	To be added	To be added	To be added	To be added
QCAZ59913	*O. verruciger*	To be added	To be added	To be added	To be added
QCAZ59915	*O. verruciger*	To be added	To be added	To be added	To be added

Museum No.	Species	Genbank Accession No.			
		12S	16S	ND1	COI
QCAZ58827	*O. verruciger*	To be added	To be added	To be added	To be added
QCAZ59126	*O. verruciger*	To be added	To be added	To be added	To be added
QCAZ58841	*O. verruciger*	To be added	To be added	To be added	To be added
QCAZ59128	*O. verruciger*	To be added	To be added	To be added	To be added
QCAZ58826	*O. verruciger*	To be added	To be added	To be added	To be added
QCAZ58833	*O. verruciger*	To be added	To be added	To be added	To be added
QCAZ58831	*O. verruciger*	To be added	To be added	To be added	To be added
QCAZ59127	*O. verruciger*	To be added	To be added	To be added	To be added
QCAZ56026	*O. vilmae*	To be added	To be added	To be added	To be added
QCAZ51205	*O. vilmae*	To be added	To be added	To be added	To be added
QCAZ54274	*O. vilmae*	To be added	To be added	To be added	To be added

Table 4. Pairwise genetic distances (uncorrected p) of 16S DNA sequences among *Osteocephalus verruciger-cannatellai* complex.

	***O. sangay* sp. n. (Clade A)**	***O.* cf. *cannatellai* (Clade B)**	***O. cannatellai* (Clade C)**	***O.* cf. *verruciger* (Clade D)**	***O.* cf. *verruciger* (Clade E)**	***O. verruciger* s. str. (Clade F)**
***O. sangay* sp. n. (Clade A)**	0					
***O.* cf. *cannatellai* (Clade B)**	0.007	0				
***O. cannatellai* (Clade C)**	0.009 ± 0.004 (0.005–0.012)	0.009 ± 0.005 (0.007–0.013)	0.001			
***O.* cf. *verruciger* (Clade D)**	0.011	0.012	0.011 ± 0.005 (0.008–0.015)	0		
***O.* cf. *verruciger* (Clade E)**	0.007 ± 0.001 (0.007–0.008)	0.008 ± 0.001 (0.008–0.009)	0.011 ± 0.004 (0.007–0.015)	0.007 ± 0.001 (0.007–0.008)	0.001	
***O. verruciger* s. str. (Clade F)**	0.013	0.015	0.015 ± 0.003 (0.013–0.017)	0.011	0.010 ± 0.001 (0.009–0.011)	0

Appendix 1. Examined specimens.

Osteocephalus cannatellai. ECUADOR: NAPO PROVINCE: Reserva Ecológica Yachana (0.84575°S, 77.22872°W), 317 m (QCAZ 48797); ORELLANA PROVINCE: San José de Payamino (0.48169°S, 77.29633°W), 285 m (QCAZ 56646); Comunidad Sinchichicta, Río Napo, Pad 16 (0.68041°S, 75.75683°W), 202 m (QCAZ 57929); PASTAZA PROVINCE: Villano B, Campo Villano, Bloque 10-Agip Oil (1.45338°S, 77.44171°W), 393 m (QCAZ 56636); Comunidad Kurintza, Campo Villano, Bloque 10-Agip Oil (1.50919°S, 77.51327°W), 269 m (QCAZ56371); Río Bobonaza (1.74611°S, 77.43720°W), 325 m (QCAZ 52767); ZAMORA CHINCHIPE PROVINCE: Centro Shuar Yawi (4.44148°S, 78.64934°W), 935 m (QCAZ 31047, 31051, 31053); Reserva Natural Maycu (4.20896°S, 78.63527°W), 882 m (QCAZ 67133).

Osteocephalus mutabor. ECUADOR: PASTAZA PROVINCE: Centro Ecológico Zanjarajuno, Río Pucayacu (1.37213°S, 77.85224°W), (QCAZ36935); Parque Nacional Llanganates, Comunidad Zarentza (1.36263°S, 78.05820°W), 1350 m (QCAZ 59900, 58892, 59899).

Osteocephalus verruciger. ECUADOR: MORONA SANTIAGO PROVINCE: Comunidad 9 de Octubre (2.22543°S, 78.26811°W), 1588 m (QCAZ 62213); Parque Nacional Sangay, Sardinayacu (2.07378°S, 78.21847°W), 1795 m (QCAZ 58808, 58826–28, 58831, 58833, 58838, 58841, 58847–48, 59126–59128); NAPO PROVINCE: Río Pucuno, sendero Pacto Sumaco-Volcán Sumaco (0.63391°S, 77.59228°W), (QCAZ 41109–10, 4113–15, 41152, 41154); Pacto Sumaco, vertiente E del Volcán Sumaco (0.56969°S, 77.59412°W), 1570 m (QCAZ1560, 1562); Sumaco, 1800 m (QCAZ8964); WildSumaco (0.67610°S, 77.59932°W), (QCAZ 57342, 62032); Bosque Protector "La Cascada" (0.14572°S, 77.49593°W), 1435 m (QCAZ 54619); PASTAZA PROVINCE: Parque Nacional Llanganates, Comunidad Zarentza (1.35644°S, 78.05807°W) 1367 m (QCAZ 59908, 59913, 59915–16, 59919, 59932, 59935–36); SUCUMBIOS PROVINCE: Hostería El Reventador (0.07374°S, 77.59327°W), 1881 m (QCAZ 52341, 66712–15, 66717–18). GERMANY: BERLIN: National History Museum, Leibniz Institute for Evolutionary and Biodiversity Research, “Ecuador” (ZMB 16589).

Osteocephalus vilmae. ECUADOR: ORELLANA PROVINCE: Comunidad Boamano, Río Araña (1.25374°S, 76.37248°W), 211 m (QCAZ 54274); PASTAZA PROVINCE: Lorocachi (1.62525°S, 75.99035°W), 214 m (QCAZ 56026).

Appendix 2. Primers used for DNA amplification.

Gen	Primer	Primer sequence	Authors
12S	MVZ59	AGGCCACTCTTGTGGGTGGT	Goebel et al. (1999)
12S	MVZ50	AACTGCCTRTTGTCCCCTGGTAT	Goebel et al. (1999)
12S	t-Met-frog	GAAGCGCCTGAACAGTTTATTAC	Wiens et al. (2005)
12S	16S-frog	TAAACTTCAGGGTGACCAAAR	Wiens et al. (2005)
12S	WL379	TTG GGG TAT GGG CCC AAA AGC T	Moen & Wiens (2008)
12S	WL379b	GAGRATTCAAATCCTCTCGTTAACTTTGAA	Moen & Wiens (2008)
12S	t-Val-frog	GGCTGTCTGTTTGCATCTTG	Wiens et al. (2005)
12S	t-Phe-frog	CCG GTC TGA ACT CAG ATC ACG	Wiens et al. (2005)
16S	16L19	ATTTTTCGTAGTTGGGTTTGRTT	Hedges et al. (2008)
16S	16Sbr-H	GCACTAGCAATAATTATYTGAACBCC	Palumbi et al. (1991)
ND1	WL379	TTGGGGTATGGGCCCAAAAGCT	Moen & Wiens (2008)
ND1	WL384	GAAGTGGAAGCCGAAGCAGSWYTGCATCAT	Moen & Wiens (2008)
ND1	t-Met-frog	GAAGCGCCTGAACAGTTTATTAC	Wiens et al. (2005)
ND1	16S-frog	TAAACTTCAGGGTGACCAAAR	Wiens et al. (2005)
CO1	dgLCO1490	GCCACTCTTGTGGGTGGTCCAT	Folmer et al. (1994)
COI	dgHCO2198	TAAACTTCAGGGTGACCAAARAAYCA	Folmer et al. (1994)

Gen	Primer	Primer sequence	Authors
COI	LCO1490	ATTTTRTCRATATCHGAGTTTGT	Folmer et al. (1994)
COI	HCO2198	ACAGAAYTAACYAACTGACT	Folmer et al. (1994)

Appendix 3. Original description of *Hyla verrucigera* by Werner (1901).

Hyla verrucigera nov. spec.
Relative with *H. hucldeyi* and *H. leprieuri*.

Tongue behind clearly free and notched, circular. Toothed palate between the back halves of the choanae, forming a figure in shape of \ /. Depressed (flat) head, as long as wide, wider than body. Rounded snout, $1–1^{1}/_{2}$ times as long as diameter of the eye. Loreal region curved, concave. Snout edge clearly, almost straight. Tympanum very clearly, approximately half the width of the ocular diameter; on this a strong fold. Interorbital space twice as wide as upper eyelid.

Three external fingers of the hand with one third palmate. Lacking pollex rudiment. Natatorial membranes of toes only reach in the fourth finger until the base of the penultimate, otherwise until the last phalanx. Discs of fingers slightly smaller than tympanum, on toes only half as wide. Posterior legs reach nostrils and one eye with the tibial joint.

Dorsal surfaces of head, trunk and back legs (except the thighs) strongly tuberculated. Anterior legs, dorsal and ventral thighs smooth, granulated only in the thorax and venter. Body sides are also smooth, clearly distinct from the tuberculated dorsum. Dark brown dorsum, monochromatic. Ventral part light brown, dirty white venter, black brown mottled.

Total length of 51 mm.

I have two copies, a larger one (female) and a juvenile.